WMCAUS
www.wmcaus.org

6th WMCAUS 2021
World Multidisciplinary Civil Engineering · Architecture · Urban Planning Symposium
30 August-3 September, 2021 - Prague (Czech Republic)

LOGO / Name of Univ./Institute

EFFECT OF NON-METALLIC COMPOSITE REINFORCEMENT ON LOAD-BEARING CAPACITY

Justyna SOBCZAK-PIĄSTKA[1], Sofiya BURCHENYA[2], Yuriy FAMULYAK[2]

[1]UTP University of Science and Technology, Faculty of Civil and Environmental Engineering and Architecture,
Al. prof. S. Kaliski Str. 7, 85-796 Bydgoszcz, Poland

[2]Lviv National Agrarian University, Faculty of Civil Engineering and Architecture,
80381, V. Velykoho Str., Dublyany, Zhovkva district, Lviv region, Ukraine

Introduction

It is known that non-metallic composite reinforcement was invented in the 60's of the last century, and already then, a large number of scientists began to investigate its physical and mechanical characteristics. Despite its rather old age, this reinforcement has not been sufficiently studied for its work in building structures. The distinctive features of work of fiberglass composite reinforcement in bending spacer elements are still insufficiently studied, which in design and production practices leads to the non-use of such reinforcement in the construction of elements of buildings and structures. The purpose of this study is to investigate the load-bearing capacity and deformability of a spacer element reinforced with non-metallic composite reinforcement. The obtained results are compared with the results of studies of a spacer element reinforced with metal rod reinforcement.

Material and Methods

To accomplish this task, two test specimens B-1 and B-2 were designed and manufactured with a cross section of 80x150 mm, a length of 1500 mm and a design span of 1300 mm. In the test specimen B-1, longitudinal working reinforcement was made of two metal rods $\varnothing 8$ class A400S, in B-2 - two fiberglass rods $\varnothing 8$ AKS 600. The longitudinal reinforcement of the compressed zone and the transverse reinforcement of both specimens was reinforcement $\varnothing 6.5$mm class A-240S. The longitudinal reinforcement of the compressed zone and the elongated zone and transverse integration into the spatial frameworks by means of the knitting wire BP-1, which reinforced the bending elements (figure 1). The production of test specimens was carried out under laboratory conditions. Three concrete cubes with a rib size of 100 mm were manufactured simultaneously with the production of the specimens. Concrete for the production of test specimens was planned in class C16/20, after testing the cubes, the average value of the cubic strength corresponded to the concrete class C8/10 and was fck,cube = 10 MPa. The study of the bending specimens was carried out on a special metal stand, where the loading was performed by two symmetric concentrated forces applied to the upper face of the beam specimen (figure 2).

Figure 1. Spatial frameworks: (a) spatial framework of test specimen B-1; (b) the spatial framework of test specimen B-2.
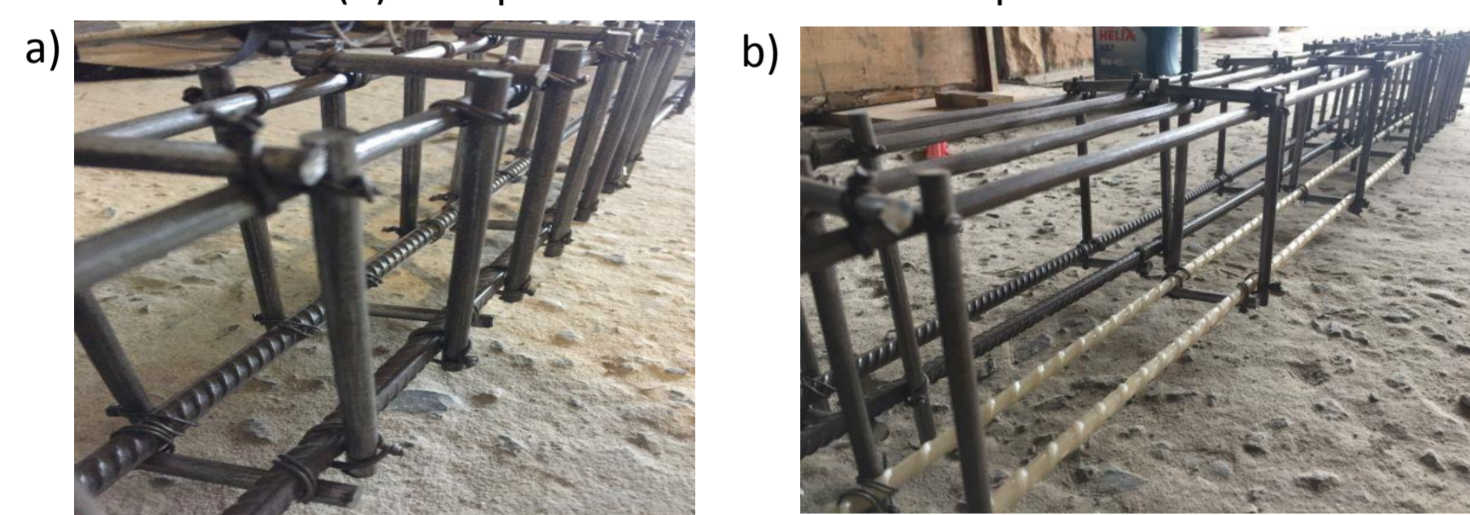

Figure 2. General view of the stand

Table 1. The results of determining the characteristics of steel

Type of reinforcement	Kind of reinforcement	Cross-section size, diameter, [mm]	Cross-sectional area, A, [cm²]	Characteristic value of reinforcement resistance f_{uk} [MPa]	Modulus of elasticity of reinforcement Es x10⁵, [MPa]	Boundary relative deformation of elongation ε_{ud}
Fiberglass AKS 600	longitudinal stretched	$\varnothing 8$ (7)	0.385	600	0.55	0.270
Rod class A400C	longitudinal stretched	$\varnothing 8$	0.503	463	1.96	0.020

Results

Before carrying out the experimental study, a theoretical calculation of the test specimens was carried out based on the deformation model. The theoretical value of the fracture moments of the specimen B-2, reinforced with fiberglass reinforcement, was found as for reinforced concrete. The criterion for the formation of cracks was assumed as the value $\varepsilon_{ctu} = {-2f_{ctm}}/{E_{ck}}$. Comparison of experimental and theoretical values of fracture loads and fractures is summarized in table 2. The development of cracks and the general appearance of the test specimens at the time of fracture are shown in figure 3 and figure 4.

As the external concentrated load increased, new normal cracks emerged between the first cracks formed. The process of crack opening and growth took place gradually (see figure 3).

The destruction of the test specimen B-1 was due to the achievement of the flowability of the reinforcement, followed by the destruction of the compressed zone of concrete, and of the test specimen B-2 - due to the destruction of the compressed concrete when reaching extreme fiber deformation limit values.
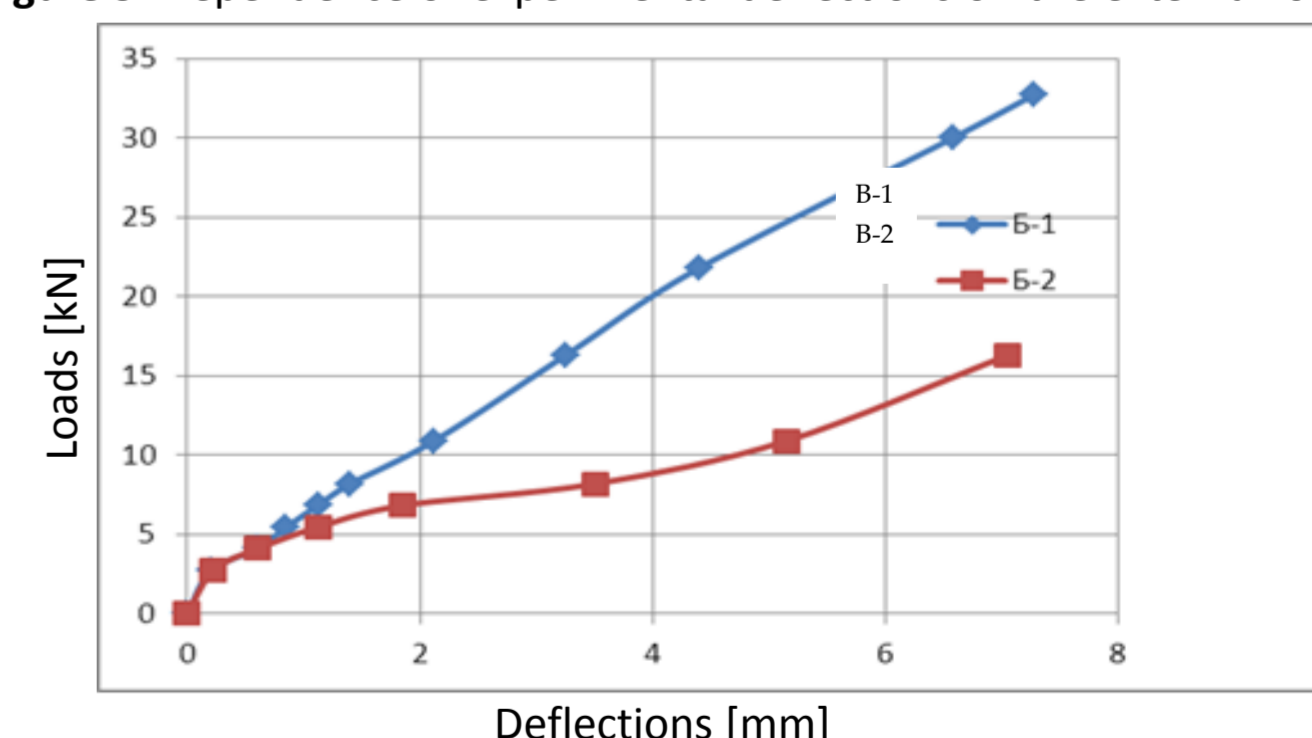

Figure 3. Creation and development of cracks in test specimens: (a) B-1; (b) B-2

Figure 5. Dependence of experimental deflections on the external load

Table 2. Experimental and theoretical values of cracks formation and fracture in test specimens

Specimen code	Experimental load at which the first cracks were formed F_{crc} [kN]	Theoretical load at which the first cracks were formed F_{crc} [kN]	Experimental load at which the specimens were destroyed F_{des} [kN]	Theoretical load at which the specimens were destroyed F_{des} [kN]
B-1	8.19	6.28	37.0	29.0
B-2	5.46	5.33	27.3	31.0

Discussions & Conclusions

The experimental study has shown the following:
1. The loads at which the first cracks in the test specimen B-1 were formed are 1.5 times higher than in the test specimen B-2.
2. The load at which the test specimens are destroyed is 1.35 times higher in the specimen B-1 compared to that of the specimen B-2.
3. The crack opening width of the specimen B-2 is almost 3 times greater than that of the specimen B-1.
4. The deformability of the test specimen B-2 is 2-2.5 times higher than that of the specimen B-1, depending on the loading level.

Acknowledgements

EcoSET
Science + Education + Technology

Uniwersytet Technologiczno-Przyrodniczy
im. Jana i Jędrzeja Śniadeckich w Bydgoszczy

AKADEMICKIE PARTNERSTWA MIĘDZYNARODOWE

NAWA
NARODOWA AGENCJA WYMIANY AKADEMICKIEJ